

Driving Style Recognition *Like* an Expert Using Semantic Privileged Information from Large Language Models

Zhaokun Chen, Chaopeng Zhang, *Student Member, IEEE*, Xiaohan Li, Wenshuo Wang, *Member, IEEE*, Gentiane Venture, *Senior Member, IEEE* and Junqiang Xi

Abstract—Existing driving style recognition systems largely depend on low-level sensor-derived features for training, neglecting the rich semantic reasoning capability inherent to human experts. This discrepancy results in a fundamental misalignment between algorithmic classifications and expert judgments. To bridge this gap, we propose a novel framework that integrates Semantic Privileged Information (SPI) derived from large language models (LLMs) to align recognition outcomes with human-interpretable reasoning. First, we introduce DriBehavGPT, an interactive LLM-based module that generates natural-language descriptions of driving behaviors. These descriptions are then encoded into machine learning-compatible representations via text embedding and dimensionality reduction. Finally, we incorporate them as privileged information into Support Vector Machine Plus (SVM+) for training, enabling the model to approximate human-like interpretation patterns. Experiments across diverse real-world driving scenarios demonstrate that our SPI-enhanced framework outperforms conventional methods, achieving F_1 -score improvements of 7.6% (car-following) and 7.9% (lane-changing). Importantly, SPI is exclusively used during training, while inference relies solely on sensor data, ensuring computational efficiency without sacrificing performance. These results highlight the pivotal role of semantic behavioral representations in improving recognition accuracy while advancing interpretable, human-centric driving systems.

Index Terms—Driving style recognition, driving behavior, semantic privileged information, large language models.

I. INTRODUCTION

RECOGNIZING driving styles plays a pivotal role in understanding human-vehicle interactions, thereby improving personalized driving experience and enhancing the acceptance of advanced driver assistance systems [1]. For example, adaptive cruise control systems offer configurable parameters, such as inter-vehicle distance, target speed, and driving modes, to accommodate both aggressive drivers prioritizing traffic throughput efficiency and conservative drivers emphasizing safety [2], [3]. Previous research has demonstrated the applicability of driving style recognition in intelligent vehicle sys-

This work was supported by the National Natural Science Foundation of China under Grant 52272411. (*Corresponding Authors: Wenshuo Wang and Junqiang Xi*).

Zhaokun Chen, Chaopeng Zhang and Xiaohan Li are with the School of Mechanical Engineering, Beijing Institute of Technology, Beijing, China (e-mail: zk.chen@bit.edu.cn; cpzhang@bit.edu.cn; lixh030114@gmail.com).

Wenshuo Wang, and Junqiang Xi are with the Division of Energy-Mobility Convergence, Beijing Institute of Technology, Zhuhai, China (e-mail: ws.wang@bit.edu.cn; xijunqiang@bit.edu.cn).

Gentiane Venture is with the Department of Mechanical Engineering, The University of Tokyo, Tokyo, Japan (e-mail: venture@g.ecc.u-tokyo.ac.jp).

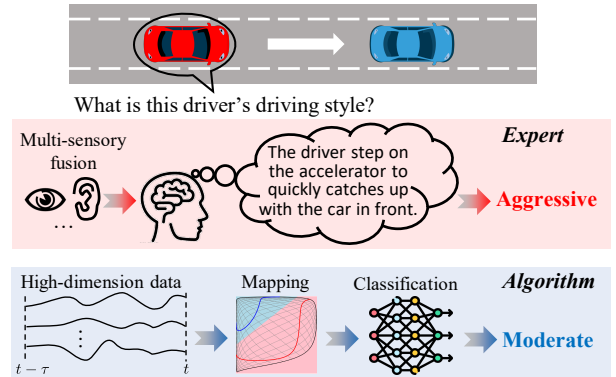


Fig. 1. The difference between an expert and an algorithm for driving style recognition.

tems including longitudinal control (e.g., personalized adaptive cruise control [4]–[6]), vertical dynamics (e.g., active suspension optimization [7]), and lateral guidance (e.g., steering assistance [8] with lane keeping [9]).

Existing approaches to driving style recognition, including rule-based [10]–[12], learning-based [13]–[16], and hybrid methods [17]), primarily rely on low-level vehicular sensor data (e.g., speed, acceleration, steering wheel angle). While these methods capture physical driving behavior, they fail to emulate the human ability to infer high-level semantic cues, such as intent, environmental context, or social interactions (Fig. 1) [18]–[20]. This semantic gap limits their capacity to model the underlying causality of driving behaviors, often resulting in misalignment between algorithmic outputs and human subjective evaluation. To bridge this gap, we argue that integrating semantically rich representations of driving behavior is essential — not only to enhance recognition accuracy but also to improve the interpretability and human-consistency of machine-generated results.

While semantic information can be manually annotated by human experts, this approach suffers from inefficiency and poor scalability, particularly for large-scale naturalistic driving datasets. Consequently, a critical challenge is the development of an automated approach capable of extracting high-quality semantic representations of driving behavior. Recent advances in Large Language Models (LLMs) have revolutionized natural language processing, demonstrating exceptional capabilities in semantic comprehension and generative tasks [21].

Leveraging these advancements, we propose DriBehavGPT, an LLM-based framework that integrates Chain-of-Thought reasoning [22] with structured prompt engineering to generate semantically rich driving behavior descriptions. The framework processes raw in-vehicle sensor data and autonomously produces semantic behavior descriptions comparable to expert human annotations. However, deploying LLMs on resource-constrained automotive electronic control units (ECUs) poses a significant challenge due to their high computational overhead and non-trivial inference latency.

To address this challenge, we propose a Learning Using Semantic Privileged Information (LUSPI) framework, which integrates LLM-generated semantic descriptions [23] with sensor data to enhance driving style recognition during training. During deployment, it operates solely on real-time CAN bus signals. This approach strikes a balance between recognition accuracy and computational efficiency, enabling feasible on-line implementation. The main contributions are twofold:

- 1) We present DriBehavGPT, an LLM-based module that automatically generates expert-like semantic descriptions of driving behaviors from in-vehicle sensor data.
- 2) We introduce a privileged information-driven learning framework that exploits SPI during training to enhance recognition accuracy while retaining real-time inference capability on embedded ECUs during deployment.

The rest of this paper is structured as follows. Section II analyzes prior work on driving style recognition using semantic information. Section III describes the LUSPI framework and theoretical underpinnings. Section IV describes real-world experiments and data collection. Section V demonstrates the experimental settings, followed by the results and analysis in Section VI and conclusions in Section VII.

II. LITERATURE REVIEW

A. Driving Behavior Semantics

Semantic cognition plays a fundamental role in interpreting complex driving behaviors, as evidenced by neuroscientific and computational studies. Semantic abstraction mechanisms analogous to linguistic understanding are activated during driving tasks [24], [25]. This insight has motivated computational approaches to encode driving behaviors into semantically meaningful patterns. Early studies relied on human-provided semantic labels (e.g., survey on overtaking [26] or speeding [27]), while recent advances employ unsupervised learning to derive interpretable representations. Wang [28] et al. decomposed car-following behaviors into 75 primitive semantic patterns using non-parametric Bayesian modeling, whereas Chen et al. [29] identified five latent semantic topics for lane-changing behaviors using latent Dirichlet allocation (LDA). Further refining this paradigm, Zhang et al. [30] introduced a hierarchical LDA to assign style-specific semantics to driving segments. Collectively, these works bridge low-level sensor data with high-level behavioral interpretations.

B. Learning Using Privileged Information (LUPI)

The Learning Using Privileged Information (LUPI) paradigm, introduced by Vapnik and Vashist [31], extends

conventional supervised learning by incorporating auxiliary knowledge (e.g., expert explanations or contextual metadata) during training. Unlike traditional frameworks where such information is discarded, LUPI leverages it to constrain the hypothesis space, often yielding superior generalization. The seminal SVM+ algorithm [31] demonstrate this by modeling slack variables via privileged features. Subsequent work validated LUPI's efficacy across domains: in computer vision, privileged descriptors improved image classification [32]–[34], disease diagnosis [35], [36], action recognition [37], [38]. For instance, in image classification, incorporating privileged information (e.g., feature descriptions provided during training) can significantly improve classifier performance [31], [39].

C. Driving Style Recognition Using Privileged Information

Although LUPI remains underexplored in driving behavior analysis, its potential is underscored by studies integrating human prior knowledge. Early rule-based systems codified expert-defined semantics (e.g., “aggressive” thresholds for acceleration), while recent work employs LLMs to extract human-aligned behavioral descriptions [40], [41]. For example, Fu et al. [40] demonstrated LLMs’ ability to annotate driving scenarios with cognitively plausible semantics, though real-world validation is pending. Hybrid approaches, such as Zhang et al.’s [17] hierarchical fusion of expert rules and data-driven models, partially leverage privileged information but decouple it from the training loop. In contrast, LUPI embeds semantic guidance directly into the learning process, offering a principled framework to unify machine learning with domain knowledge — a direction ripe for exploration in driving style recognition.

III. THE LUSPI FRAMEWORK

The proposed LUSPI framework for driving style recognition (Fig. 2) comprises three core modules: DriBehavGPT, Embedding, and LUPI. The LUPI module takes driving behavior features, style labels (Section IV), and semantic privileged information generated by the DriBehavGPT module. DriBehavGPT translates sequential driving behavior data into textual descriptions, which the Embedding module then converts into compact numerical representations. By integrating data-driven features with the semantic reasoning capabilities of LLM, LUSPI enhances both the accuracy and interpretability of driving style recognition.

A. LUPI: Support Vector Machine Plus (SVM+)

In the LUPI paradigm, training samples contain additional privileged information unavailable during testing. Formally, the training set is denoted as $\{(\mathbf{x}_i, \mathbf{x}_i^*, y_i)\}_{i=1}^n$, where n is the number of driving segments, $\mathbf{x}_i \in \mathbb{R}^D$ is the D -dimensional feature vector of the i -th segment, $\mathbf{x}_i^* \in \mathbb{R}^{D^*}$ is its associated D^* -dimensional privileged semantic information describing driving behavior, and $y_i \in \mathcal{Y} = \{\text{aggressive, moderate, conservative}\}$ is the driving style label. While standard SVM+ is a binary classifier, we extend it to multi-class classification using a one-vs.-one strategy

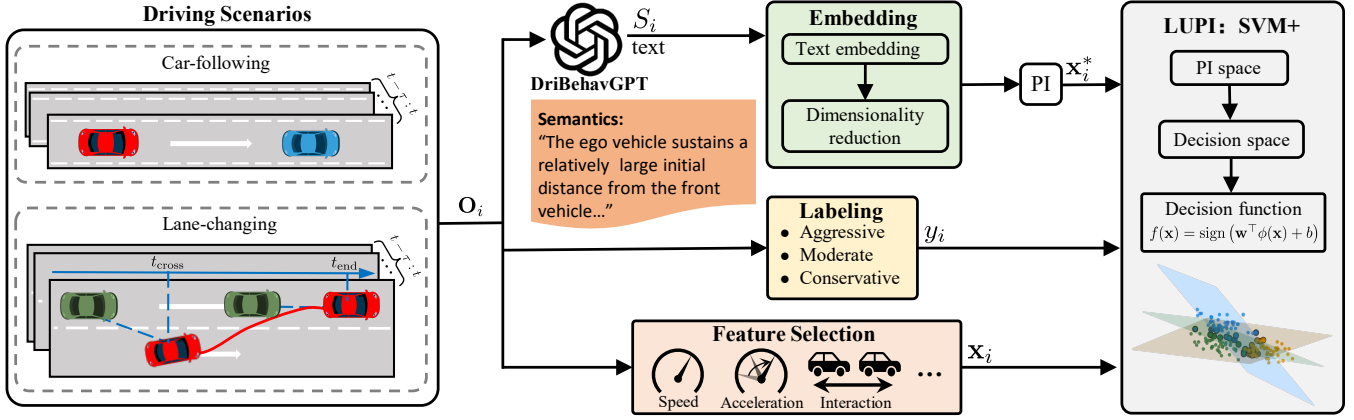


Fig. 2. The LUSPI framework for driving style recognition. The input consists of the i -th sequential driving data O_i collected from diverse scenarios (i.e., car-following and lane-changing). These data are processed by DriBehavGPT to generate driving behavior semantic descriptions S_i , which are further transformed into privileged information (PI) \mathbf{x}_i^* through text embedding and dimensionality reduction.

[42], constructing pairwise classifiers and determining final predictions through majority voting. For clarity, we present the formulation for binary classification. The goal is to learn a decision function $f(\mathbf{x}) : \mathbb{R}^D \rightarrow \mathcal{Y}$ mapping inputs to driving style labels.

Similar to SVM, Support Vector Machine Plus (SVM+) [31] defines the decision function as:

$$f(\mathbf{x}) = \text{sign}(\mathbf{w}^\top \phi(\mathbf{x}) + b) \quad (1)$$

where $\mathbf{x} = \{\mathbf{x}_i\}_{i=1}^n$, \mathbf{w} is the weight vector, b is the bias term, $\phi(\cdot)$ is a feature mapping that enhances linear separability. We obtain the decision function by optimizing \mathbf{w} and b . The standard SVM optimization problem is:

$$\begin{aligned} \min_{\mathbf{w}, b, \xi} \quad & \frac{1}{2} \|\mathbf{w}\|^2 + C \sum_{i=1}^n \xi_i \\ \text{s.t.} \quad & y_i (\mathbf{w}^\top \phi(\mathbf{x}_i) + b) \geq 1 - \xi_i, \\ & \xi_i \geq 0, \quad \forall i = 1, \dots, n \end{aligned} \quad (2)$$

where ξ_i is the slack variable for classification errors, and C controls the trade-off between margin width and classification error.

The SVM+ incorporates privileged information to refine the slack variables, leading to the following optimization:

$$\begin{aligned} \min_{\mathbf{w}^*, b^*, \mathbf{w}, b} \quad & \frac{1}{2} \|\mathbf{w}\|^2 + \frac{\gamma}{2} \|\mathbf{w}^*\|^2 + C \sum_{i=1}^n \xi(\mathbf{w}^*, b^*, \psi(\mathbf{x}_i^*)) \\ \text{s.t.} \quad & y_i (\mathbf{w}^\top \phi(\mathbf{x}_i) + b) \geq 1 - \xi(\mathbf{w}^*, b^*, \psi(\mathbf{x}_i^*)), \\ & \xi(\mathbf{w}^*, b^*, \psi(\mathbf{x}_i^*)) \geq 0, \quad i = 1, \dots, n \end{aligned} \quad (3)$$

where $\xi(\mathbf{w}^*, b^*, \psi(\mathbf{x}_i^*)) = \mathbf{w}^{*\top} \psi(\mathbf{x}_i^*) + b^*$ is a slack function defined in the privileged semantic information space, $\psi(\cdot)$ is a feature mapping for privileged data, and \mathbf{w}^* and b^* are the weight vector and bias term, respectively. SVM+ introduces the following improvements in the model architecture: (i) SVM+ replaces the slack variable ξ_i with $\xi(\mathbf{w}^*, b^*, \psi(\mathbf{x}_i^*))$ to adjust classification error tolerance based on driving semantic privileged information, improving consistency with human

subjective evaluations. (ii) SVM+ simultaneously optimizes both the driving features (governed by \mathbf{w}) and the semantic privileged data, regularized by $\frac{\gamma}{2} \|\mathbf{w}^*\|^2$, with a hyperparameter γ controlling the strength of semantic information on decision-making. This embeds human-like semantic descriptions into the geometric structure of the model and generates dynamically adaptive driving style classification boundaries.

To solve (3), we construct the Lagrangian function (Appendix A) and derive the dual form of SVM+ as:

$$\begin{aligned} \max_{\alpha, \beta} \quad & \sum_{i=1}^n \alpha_i - \frac{1}{2} \sum_{i,j=1}^n \alpha_i \alpha_j y_i y_j K(\mathbf{x}_i, \mathbf{x}_j) \\ & - \frac{1}{2\gamma} \sum_{i,j=1}^n (\alpha_i + \beta_i - C)(\alpha_j + \beta_j - C) K^*(\mathbf{x}_i^*, \mathbf{x}_j^*) \\ \text{s.t.} \quad & \sum_{i=1}^n (\alpha_i + \beta_i - C) = 0, \\ & \sum_{i=1}^n y_i \alpha_i = 0, \\ & \alpha_i \geq 0, \quad \beta_i \geq 0. \end{aligned} \quad (4)$$

where $K(\mathbf{x}_i, \mathbf{x}_j) = \phi(\mathbf{x}_i)^\top \phi(\mathbf{x}_j)$ is a kernel function for driving features, and $K^*(\mathbf{x}_i^*, \mathbf{x}_j^*) = \psi(\mathbf{x}_i^*)^\top \psi(\mathbf{x}_j^*)$ represents a kernel function for semantic privileged information. We adopt the widely-used Gaussian kernel function [43], such as $K(\mathbf{x}_i, \mathbf{x}_j) = \exp(-\lambda \|\mathbf{x}_i - \mathbf{x}_j\|^2)$, where the parameter λ determines the shape of the hyperplane.

We solve the optimization problem using the Sequential Minimal Optimization (SMO) algorithm [44] (Appendix B). From the optimal Lagrange multipliers and the stationary conditions of the Lagrangian ($\nabla_{\mathbf{w}} L = 0$, $\nabla_{\mathbf{w}^*} L = 0$), the weight vectors \mathbf{w} and \mathbf{w}^* are derived as

$$\begin{aligned} \mathbf{w} &= \sum_{i=1}^n \alpha_i y_i \phi(\mathbf{x}_i), \\ \mathbf{w}^* &= \frac{1}{\gamma} \sum_{i=1}^n (\alpha_i + \beta_i - C) \psi(\mathbf{x}_i^*) \end{aligned} \quad (5)$$

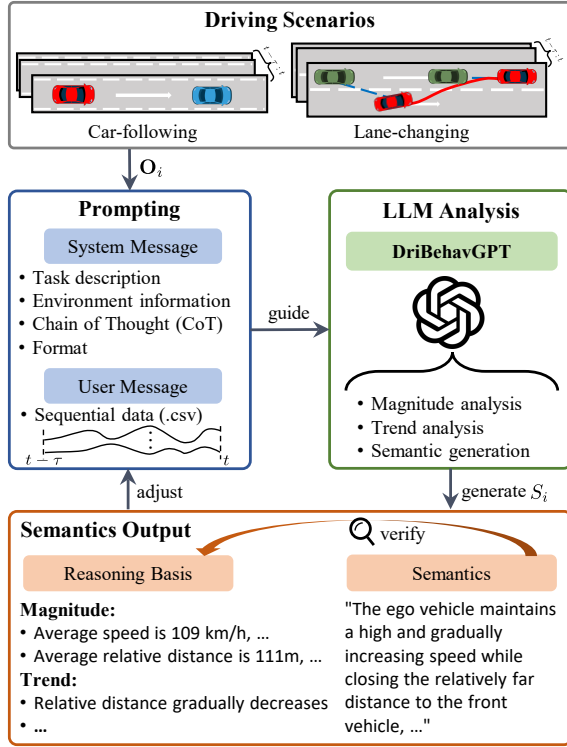


Fig. 3. DriBehavGPT for semantically describing driving behaviors.

Substituting (5) into (1) yields the decision function, which depends only on the driving features' weight vector.

$$f(\mathbf{x}) = \text{sign} \left(\sum_{i=1}^n \alpha_i y_i K(\mathbf{x}_i, \mathbf{x}) + b \right) \quad (6)$$

where the bias term b computed using all support vectors

$$b = \frac{1}{N_{SV}} \sum_{i \in SV} (y_i - \sum_{j=1}^n \alpha_j y_j K(\mathbf{x}_j, \mathbf{x}_i)) \quad (7)$$

Here, $SV = \{i \mid \alpha_i > 0\}$ denotes the set of support vector indices (i.e., driving segments influencing the decision hyperplane), and N_{SV} is their cardinality.

B. DriBehavGPT

We propose DriBehavGPT (Fig. 3), an LLM-based module to generate semantics of driving behavior. The task is formulated as a language modeling problem. Structured prompts, designed through prompt engineering, guide DriBehavGPT in translating the i -th sequential driving observations O_i (e.g., speed, acceleration, relative distance/speed) into human-interpretable semantic description S_i (e.g., 'The ego vehicle maintains a high and slightly increasing speed...'). DriBehavGPT operates under a zero-shot learning paradigm, eliminating task-specific training by leveraging pretrained LLMs such as ChatGPT-4 [45]. To ensure transparency and reliability, we integrate a Chain-of-Thought mechanism into the prompt design, enabling the model to generate semantic description alongside their analytical reasoning. This allows systematic verification and refinement of the semantic description, ensuring their alignment with the derived reasoning basis. By jointly

producing behaviors and their justification, DriBehavGPT improves interpretability, traceability, and alignment with domain knowledge with preserving the LLM's contextual understanding.

1) *Prompt Engineering*: To effectively leverage the natural language processing capabilities of LLMs, we design structured prompts for DriBehavGPT to systematically encode driving scenarios and tasks. The input prompts comprises two components: a system message, which frames the LLM's role and reasoning process, and a user message, which supplies driving data and contextual details. This dual-prompt design ensures optimal alignment between LLM capabilities and the analytical demands of driving behavior assessment.

System Message. This treats DriBehavGPT as an expert for driving behavior analysis, specifies task requirements, and employs Chain-of-Thought prompting to elicit stepwise reasoning. The message structures the analysis into three phases: First, *magnitude analysis*. Humans evaluate driving styles using perceptible quantitative features (e.g., speed and acceleration magnitude) [46]. Similarly, autonomous vehicle comfort is assessed via acceleration and jerk metrics [47]. To mirror human judgment, DriBehavGPT computes statistical features (e.g., mean speed, acceleration fluctuation range) from raw sequential driving data. Second, *trend analysis*. Human perception of driving styles relies on multisensory integration of temporal patterns [48]. Trend analysis supplements magnitude-based metrics by capturing dynamic contextual cues, enhancing holistic behavior interpretation. Finally, *semantics generation*. Combining magnitude and trend features, DriBehavGPT utilizes the LLM's comprehension and generative capabilities to translate driving sequential data into natural language descriptions.

User Message. The user message delivers formatted time-series driving data (i.e., CSV) with annotated columns to facilitate model comprehension.

2) *Interpretability of Driving Behavior Semantics*: To ensure transparency and credibility, this study integrates explicit explanatory requirements into the prompt design, guiding DriBehavGPT to furnish both semantic outputs and their analytical justifications. This approach elucidates the model's reasoning process, offering users actionable insight into its decision-making logic. Formally, the prompting-reasoning process can be defined as:

$$\{\mathcal{S}, \mathcal{R}\} = F_{\text{GPT}}(\mathcal{M}, \mathcal{U}) \quad (8)$$

where F_{GPT} denotes the DriBehavGPT module, it combines the system message (\mathcal{M}) and user message (\mathcal{U}), \mathcal{S} is the semantic description of driving behaviors, and \mathcal{R} provides the reasoning basis.

Unlike conventional methods that rely on opaque numerical features, DriBehavGPT frames driving behavior analysis as a language generation task. This paradigm shift enables human-understandable semantics (i.e., translating raw data into intuitive behavioral descriptors), traceable reasoning (i.e., exposing the causal linkages between data features and semantic conclusions), and dynamic interpretability (i.e., revealing how behavioral characteristics evolve temporally).



Fig. 4. The driving routes of experiments in Changchun, China.

C. Embedding

1) *Text Embedding*: To process textual data with SVM+, we convert semantic descriptions into numerical representations using text embedding techniques. We employ SentenceTransformers [49] to generate contextualized embeddings that capture the semantics of driving behavior, ensuring compatibility with SVM+. The SentenceTransformers leverages transformer-based architectures to produce context-aware representations that capture rich intra- and inter-sentence relationships than traditional static word embeddings (e.g., Word2Vec [50], GloVe [51]), yielding discriminative and semantically rich embeddings.

2) *Dimensionality Reduction*: The embeddings generated by SentenceTransformers typically have high dimensionality (several hundred dimensions), which may introduce computational inefficiency and feature redundancy. To address this, we implement Uniform Manifold Approximation and Projection (UMAP) [52] for dimensionality reduction. Compared to alternative techniques (e.g., Principal Component Analysis and t-distributed Stochastic Neighbor Embedding), UMAP preserves both local and global structures in the data while efficiently handling nonlinear feature distributions. This ensures stable and compact representations of the semantic embeddings, which we then extract as privileged information \mathbf{x}_i^* for SVM+.

IV. DATA COLLECTION AND DRIVING STYLE LABELING

This section presents the methodology for data collection and driving style annotation in car-following and lane-changing scenarios. Car-following data were acquired using an instrumented test vehicle, while lane-changing data were sourced from the publicly available highD [53] dataset. A unified annotation framework was applied to both datasets to ensure consistency in driving style labeling.

A. Car-following Data

1) *Driving Experiment*: To collect real human driving behavior data for method validation, we conducted large-scale naturalistic driving experiments involving 100 participants across diverse demographics (occupation, gender, age: 21 ~ 60 years, and driving experience: 1 ~ 35 years). Detailed participant statistics are available in [30]. Experiments were performed on a 40.2 km highway stretch (Fig. 4)

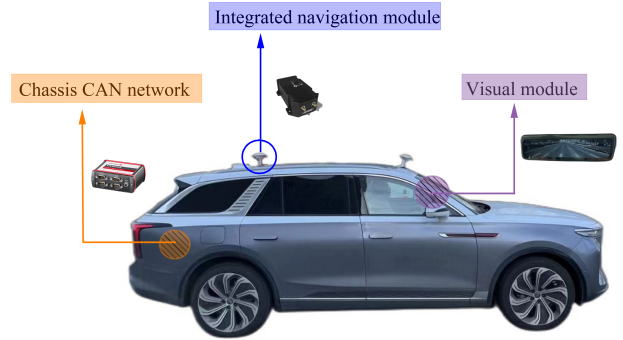


Fig. 5. The testing vehicle equipped with a data-acquisition system.

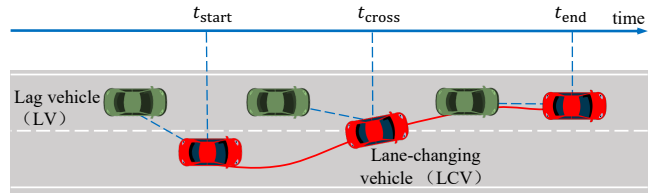


Fig. 6. Illustration of key time-point in lane-changing behavior definition.

in Changchun, China. Participants operated the test vehicle (Fig. 5) with a data acquisition system. The data acquisition system consists of three modules: the chassis CAN network for vehicle dynamics (speed, acceleration), an integrated navigation module for positioning, and a vision module for front-vehicle detection and relative distance estimation. This setup enabled recording of critical signals for car-following event extraction and driving style characterization.

2) *Car-following Events Extraction*: To extract the car-following events, we selected four variables according to [54]–[56]: Relative distance (Δd_t^{EV}) between the ego vehicle (EV) and front vehicle (FV), relative speed (Δv_t^{EV}) between the FV and the EV, ego vehicle speed (v_t^{EV}), ego vehicle longitudinal acceleration ($a_{lon,t}^{EV}$). The car-following events were extracted from the collected data under the following conditions [57]. After filtering, 628 car-following segments were retained for analysis.

3) *Feature Representation*: Driving styles were characterized using segment-wise mean values of kinematic features, ensuring computational efficiency and real-time applicability. The feature vector $\mathbf{x}_i^{cf} \in \mathbb{R}^3$ for the i -th car-following segment is:

$$\mathbf{x}_i^{cf} = \text{mean}\{v_{\tau_i}^{EV}, a_{lon,\tau_i}^{EV}, \text{TTC}_{\tau_i}\}^T \quad (9)$$

where $\text{mean}\{\cdot\}$ computes element-wise averages over the segment, $\text{TTC}_t = \Delta d_t^{EV} / \Delta v_t^{EV}$ is the time-to-collision (TTC) at time t , τ_i is the duration of the i -th segment.

B. Lane-changing Data

1) *Definition of Lane-changing Events*: To automate lane-changing detection from large-scale trajectory data, we define

a lane-change maneuver as a complete lateral transition into an adjacent lane, segmented by three critical timestamps (Fig. 6) [58], [59]: (i) Start time (t_{start}) — The instant when the vehicle’s lateral velocity first exceeds 0.34 m/s [60], marking the transition from lane-keeping to lane-changing initiation. (ii) Crossing time (t_{cross}) — The moment when the vehicle’s centerline crosses the lane boundary. (iii) End time (t_{end}) — The time at which the lateral speed decays below 0.2 m/s, indicating maneuver completion.

2) *Lane-changing Events Extraction*: Following [58], [61], we defined the lane-changing event extraction procedure based on behavioral completeness and interaction with a following vehicle. The extraction process comprises four steps. (i) **Key time points identification**: For each lane-changing event, we extract the timestamps t_{start} , t_{cross} , and t_{end} (defined in Section IV-B1) and record the full trajectory of the lane-changing vehicle over the interval $[t_{\text{start}}, t_{\text{end}}]$; (ii) **Following vehicle assignment**: The lag vehicle is identified as the one spatially closest to the rear of the lane-changing vehicle at t_{end} and its ID is stored for analysis; (iii) **Event completeness validation**: Ensure that the lag vehicle remains within the recording range and stays in the same lane throughout $[t_{\text{start}}, t_{\text{end}}]$; (iv) **Interaction validation**: To ensure meaningful interaction, [60], only events where the time headway at t_{cross} is less than two seconds are retained. Applying this procedure to the highD dataset yields 633 valid lane-changing events for further analysis.

3) *Lane-changing Feature Selection*: Based on prior research [62], [63], we characterize the lane-changing style from two aspects: (i) the relative motion between vehicles and (ii) the lateral control of the lane-changing vehicles. We consider the following variables: relative distance (Δd_t^{LCV}) and relative speed (Δv_t^{LCV}) between the lane-changing vehicle (LCV) and the lag vehicle in the target lane, and LCV’s lateral acceleration ($a_{\text{lat},t}^{\text{LCV}}$). These variables provide intuitive physical interpretations of driving styles: Conservative drivers maintain larger inter-vehicle gaps, respond more promptly, and exhibit smoother lateral movements, while aggressive drivers tend to adopt smaller gaps, exhibit delayed evasive actions, and apply more abrupt steering. We used the mean values of the above variables within the segment as the features. For the feature vector of the i -th lane-changing segment \mathbf{x}_i^{lc} , we represent it using the mean values of these variables over the segment duration τ_i^{lc} :

$$\mathbf{x}_i^{\text{lc}} = \text{mean}\{\Delta d_{\tau_i^{\text{lc}}}^{\text{LCV}}, \Delta v_{\tau_i^{\text{lc}}}^{\text{LCV}}, a_{\text{lat},\tau_i^{\text{lc}}}^{\text{LCV}}\}^{\top}. \quad (10)$$

C. Driving Style Labeling

1) *Car-following Style Labeling*: Three primary methods exist for driving style annotation: manual labeling, rule-based classification, and clustering techniques. Manual annotation ensures high accuracy but is labor-intensive, while rule-based methods are computationally efficient but lack adaptability. Clustering techniques balance between automation and flexibility. To leverage their strengths, we propose a three-stage annotation pipeline (Fig. 7), which processes car-following data sequentially through the following steps: (i) **Rule-based**

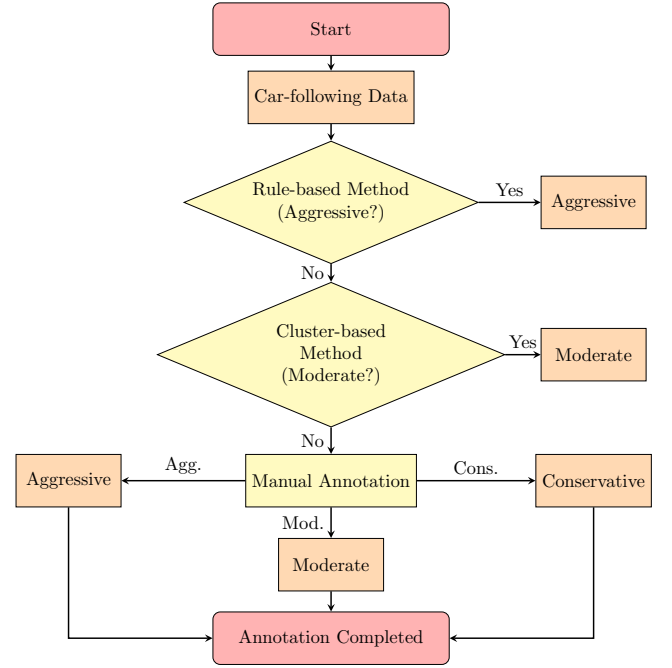


Fig. 7. Three-stage annotation workflow for driving style labeling.

aggressive style detection: Aggressive driving styles are identified by thresholding two critical variables: speed and TTC. Samples exceeding 120 km/h (the legal highway limit in the data collection region) or with $\text{TTC} < 5\text{s}$ [64] are labeled as aggressive. (ii) **Clustering-based moderate style identification**: For samples not classified as aggressive, we apply DBSCAN clustering [65] to distinguish moderate driving style with vehicle speed, acceleration, and TTC. (iii) **Manual annotation**: The remaining unclassified samples are labeled by four independent annotators with domain expertise. Each sample is categorized based on majority voting, ensuring consistency. The pipeline labeled 183 aggressive, 307 moderate, and 138 conservative car-following samples.

2) *Lane-Changing Style Labeling*: The lane-changing data are annotated using the three-stage driving style labeling procedure (Section IV-C1). Based on statistical analysis of the lane-changing dataset and insights from [62], we define the following classification criteria. A lane-changing sample is labeled as aggressive if it satisfies at least one of the following conditions: Average relative distance to the preceding vehicle $< 20\text{ m}$, average relative speed $< 0\text{ m/s}$ (indicating closing-in behavior), or average lateral acceleration $> 0.5\text{ m/s}^2$ (reflecting abrupt steering maneuvers). Samples not classified by the rule-based criteria were annotated using clustering and manual verification. The final labeled dataset comprises 216 aggressive, 313 moderate, and 104 conservative lane-changing samples.

V. EXPERIMENTAL SETTINGS

We evaluate the proposed method in car-following and lane-changing scenarios. Below, we detail the prompt design for DriBehavGPT, the parameter configuration of the LUSPI module, and the evaluation metrics for both scenarios.

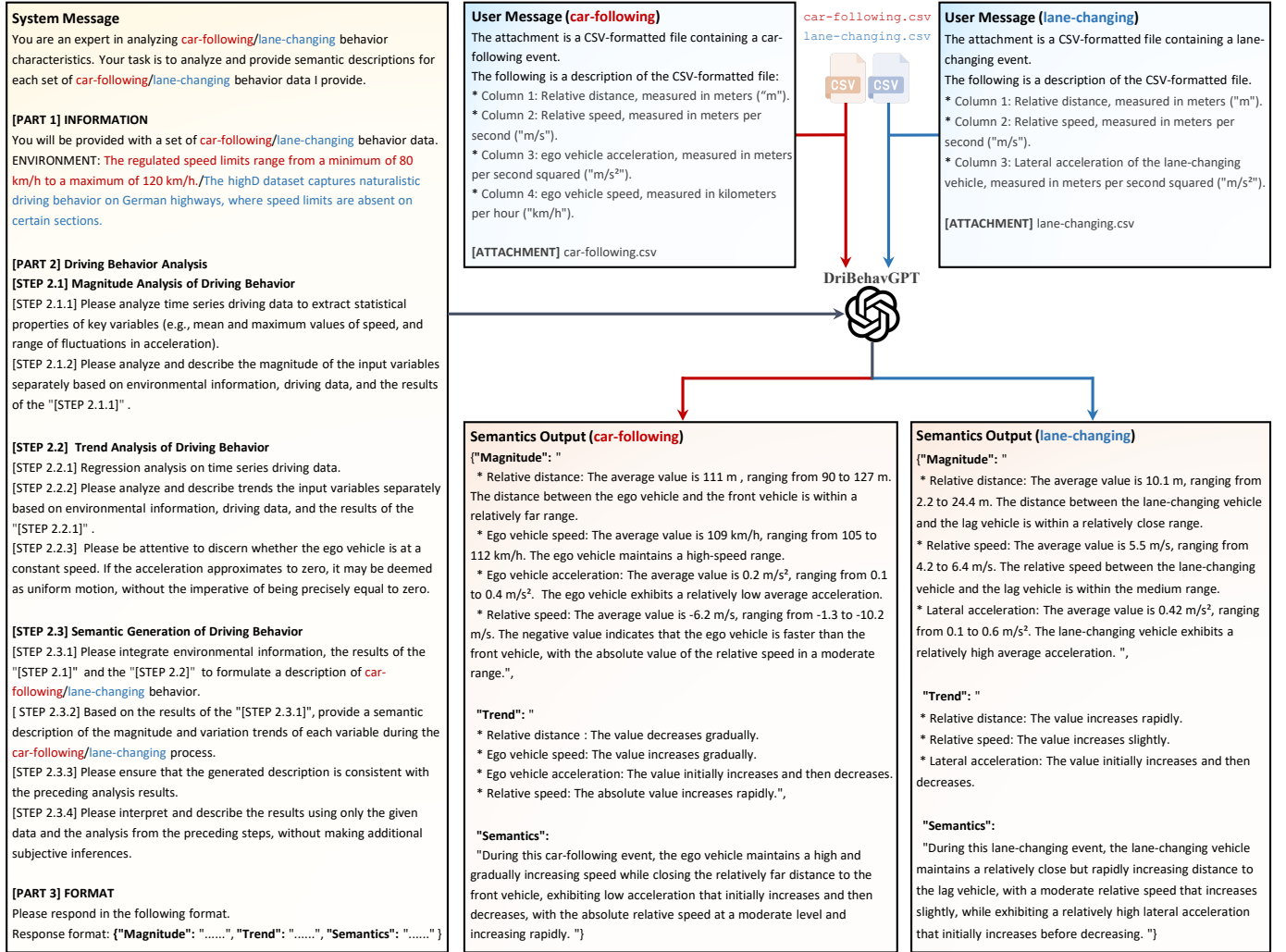


Fig. 8. Prompt design for DriBehavGPT in car-following (red mark) and lane-changing (blue mark) scenarios.

A. Prompt Design for DriBehavGPT

To extract car-following and lane-changing behavior semantics using large language models, we design scenario-specific prompts (Fig. 8).

1) *Car-following Scenario*: To accurately characterize dynamic car-following behaviors, DriBehavGPT integrates four dynamic features: (i) Ego vehicle (EV) speed sequence ($v_{\tau_i}^{EV}$), which reflects the driver's speed preference, (ii) Ego vehicle acceleration sequence (a_{lon, τ_i}^{EV}), which captures the driver's acceleration habits, (iii) Relative distance sequence ($\Delta d_{\tau_i}^{EV}$), which depicts the inter-vehicle gap dynamics, indicating risk tolerance, and (iv) Relative speed sequence ($\Delta v_{\tau_i}^{EV}$), which describes the relationship between the two vehicles. These features are transformed into semantic descriptions using a large language model. The input-output structure is

$$\text{Input: } \mathbf{O}_i^{cf} = [v_{\tau_i}^{EV}, a_{lon, \tau_i}^{EV}, \Delta d_{\tau_i}^{EV}, \Delta v_{\tau_i}^{EV}]$$

$$\text{Output: } S_i^{cf}$$

where S_i^{cf} is a text-based semantic description of the i -th car-following segment.

The user message provides the car-following time-series data (e.g., in CSV format, such as *car-following.csv*), with explicit column-wise descriptions (including units) to ensure precise interpretation. The system message follows the approach in Section III-B1, encompassing environmental context, behavior magnitude/trend analysis, semantic generation guidelines, and output formatting rules. The combined system message, user message, and input data constitute the structured prompt, which is processed by DriBehavGPT to generate human-interpretable behavior semantics.

2) *Lane-changing Scenario*: DriBehavGPT captures dynamic lane-changing behaviors using three key features: (i) Relative distance sequence ($\Delta d_{\tau_i}^{LCV}$), which captures the safety gap evolution between the lane-changing vehicle (LCV) and the lag vehicle (LV) in the target lane, (ii) Relative speed sequence ($\Delta v_{\tau_i}^{LCV}$), which describes interaction dynamics between the LCV and the LV, and (iii) Lateral acceleration sequence (a_{lat, τ_i}^{LCV}), which represents the sharpness of steering maneuvers. These time-series features are processed by LLM to generate semantic descriptions. The model's input and

TABLE I
MODELS AND PARAMETERS OF MODULES IN THE LUSPI FRAMEWORK.

LUSPI Module	Model	Parameters
DriBehavGPT	OpenAI GPT-4o	-
Text Embedding	SentenceTransformers	all-mpnet-base-v2
Dimensionality Reduction	UMAP	n_components= 5
LUPI	SVM+	cf: $C = 8, \gamma = 1.1$ lc: $C = 13, \gamma = 1.3$

output are defined as:

$$\text{Input : } \mathbf{O}_i^{\text{lc}} = \left[\Delta a_{\tau'_i}^{\text{LCV}}, \Delta v_{\tau'_i}^{\text{LCV}}, a_{\text{lat}, \tau'_i}^{\text{LCV}} \right]$$

$$\text{Output : } S_i^{\text{lc}}$$

where S_i^{lc} is the text-based semantic description of the i -th lane-changing segment.

We employ a similar prompt structure for the lane-changing scenario. The user message provides specific lane-changing behavior data in CSV format (i.e., `lane-changing.csv`), complete with explicit column descriptions to maintain interpretability. Meanwhile, the system message retains the same analytical framework as described previously, allowing DriBehavGPT to generate corresponding behavior semantics for this different driving context.

B. LUSPI Module Parameters and Baseline Method

We present the models and core parameters of the four modules in the LUSPI framework (Table I). DriBehavGPT is constructed using OpenAI’s GPT-4o API. To ensure adaptability, we adopt a zero-shot approach via prompt engineering, rather than fine-tuning. Text embeddings are generated using SentenceTransformers [49], which encodes semantic descriptions of car-following events into vectorized representations. For computational efficiency, we reduce embedding dimensionality using the UMAP method [52]. A grid search strategy optimizes the hyperparameters (C , γ). We adopt support vector machines (SVM) as the baseline for driving style recognition. A grid search optimizes hyperparameters, and we evaluate SVM alongside LUSPI using identical five-fold cross-validation protocols to ensure a fair comparison.

C. Evaluation Metrics

We evaluate the performance of the proposed LUSPI method and SVM using four standard metrics: precision, recall, F_1 -score, and accuracy. To formulate these metrics for each driving style categories, we use an integer iterator z , where $z = 1$ corresponds to conservative, $z = 2$ to moderate, and $z = 3$ to aggressive. We define $n_{\text{true}}(z)$ as the number of ground-truth samples of the z -th category, $n_{\text{pred}}(z)$ as the number of samples classified as the z -th category, and $n_{\text{correct}}(z)$ as the number of correctly predicted samples for the z -th category. The metrics are defined as follows.

- Precision ($\eta_{\text{pre},z}$) measures the model’s reliability in minimizing false positives — i.e., misclassifying other styles as the z -th category,

$$\eta_{\text{pre},z} = \frac{n_{\text{correct}}(z)}{n_{\text{pred}}(z)}. \quad (11)$$

- Recall ($\eta_{\text{rec},z}$) quantifies the model’s ability to avoid false negatives by capturing most instances of the z -th category,

$$\eta_{\text{rec},z} = \frac{n_{\text{correct}}(z)}{n_{\text{true}}(z)}. \quad (12)$$

- F_1 -score (F_1) represents the harmonic mean of precision and recall, balancing the trade-off between false positives and false negatives. We report the macro-average across all styles,

$$F_1 = \frac{1}{3} \sum_{z=1}^3 \left(\frac{2\eta_{\text{pre},z}\eta_{\text{rec},z}}{\eta_{\text{pre},z} + \eta_{\text{rec},z}} \right). \quad (13)$$

- Accuracy (η_{acc}) is the overall proportion of correctly classified segments,

$$\eta_{\text{acc}} = \frac{\sum_{z=1}^3 n_{\text{correct}}(z)}{n} \quad (14)$$

where n is the total number of tested segments (car-following or lane-changing).

VI. EXPERIMENTAL VERIFICATION AND RESULT ANALYSIS

A. Overall Performance

As summarized in Table II, the proposed LUSPI method achieves superior performance compared to the SVM baseline in both scenarios. In the car-following task, LUSPI attains 90.1% accuracy and a 90.2% F_1 -score, representing improvements of 7.1% and 7.6% over SVM, respectively. Notably, it demonstrates balanced gains in both precision and recall across different driving styles. For conservative driving behaviors, LUSPI attains 94.1% precision (5.6% higher than SVM) and 91.3% recall (10.5% higher than SVM), indicating more reliable identification of cautious driving patterns with fewer false positives. The improvements extend to moderate and aggressive driving styles, achieving 90.3% precision (7.4% above SVM) and 87.4% recall (a 10.4% improvement over SVM), respectively, confirming its robustness in distinguishing subtle behavioral variations.

Similarly, in the lane-changing scenario, LUSPI achieves 91.5% accuracy (a 7.0% improvement over SVM) and a 91.1% F_1 -score (a 7.9% improvement over SVM), further validating its generalization capability. For conservative lane changes, precision improves by 11.1% (92.8%) and recall by 11.0% (86.5%), while moderate styles exhibit a 6.9% gain in recall (94.6%). Importantly, aggressive lane changes are detected with 93.7% precision (an 8.1% improvement over SVM), demonstrating high reliability in recognizing risky maneuvers.

The consistent and significant improvements across all metrics and scenarios highlight LUSPI’s robustness and adaptability. Unlike traditional methods that often suffer from a precision-recall trade-off, LUSPI simultaneously enhances both, ensuring reliable performance in real-world applications. Its balanced efficiency across conservative, moderate, and aggressive driving styles confirms its capability to handle diverse behavioral patterns in dynamic environments. Furthermore, the stable performance gains (ranging from 5% to over 11%)

TABLE II
THE PERFORMANCE COMPARISON BETWEEN THE LUSPI FRAMEWORK AND THE SVM BASELINE IN CAR-FOLLOWING AND LANE-CHANGING SCENARIOS

Driving scenario	Driving style	Precision		Recall		Accuracy		F ₁ -Score	
		LUSPI	SVM	LUSPI	SVM	LUSPI	SVM	LUSPI	SVM
Car-following	Conservative	94.1%	89.1%	91.3%	82.6%	90.1%	84.1%	90.2%	83.8%
	Moderate	90.3%	84.1%	91.2%	87.6%				
	Aggressive	87.0%	80.6%	87.4%	79.2%				
Lane-changing	Conservative	92.8%	83.5%	86.5%	77.9%	91.5%	85.5%	91.1%	84.4%
	Moderate	89.7%	85.2%	94.6%	88.5%				
	Aggressive	93.7%	86.7%	89.4%	84.7%				

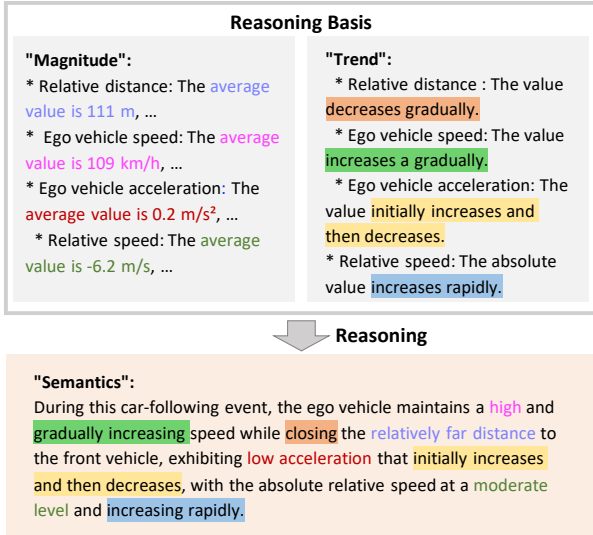


Fig. 9. Illustration of chain-of-thought reasoning by DriBehavGPT in a car-following scenario.

suggest strong generalization potential for unseen driving conditions—an essential factor for real-world deployment. These results validate that leveraging privileged information during training significantly enhances the model’s ability to discern fine-grained driving behaviors, making LUSPI a promising approach for practical intelligent transportation systems.

B. Interpretability of DriBehavGPT

The key advantage of DriBehavGPT lies in its structured analytical framework, which generates semantic, interpretable, and traceable outputs through step-by-step reasoning. By decomposing complex driving decisions into human-understandable logical chains, the model provides transparent and explainable behavior analysis, effectively bridging the gap between black-box models and user cognition.

1) *Car-following Scenario*: DriBehavGPT generates interpretable explanations in car-following scenarios by combining magnitude and trend analysis. As illustrated in Fig. 9, the model’s semantic outputs are both descriptive and quantifiably grounded. For magnitude analysis, it captures static behavioral traits — e.g., “relatively far distance to the front vehicle” is validated by “average relative distance of 111 m”, and “high-speed travel” is supported by “average speed of 109 km/h”. For trend analysis, it underpins dynamic behavioral changes — e.g., “relative distance

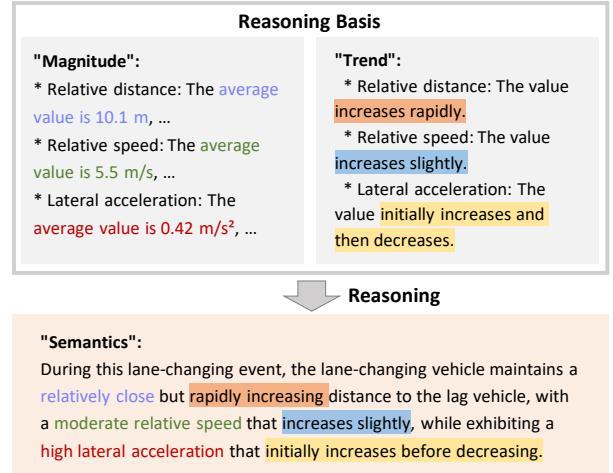


Fig. 10. Illustration of chain-of-thought reasoning by DriBehavGPT in a lane-changing scenario.

gradually decreasing” indicates closing proximity to the leading vehicle and “speed gradually increasing” suggests progressive acceleration. These analyses jointly enrich feature interpretation — e.g., a negative relative speed with an increasing absolute value implies the ego vehicle is accelerating faster than the front vehicle, reinforcing the semantic explanation. This dual-faceted reasoning ensures outputs are not only human-readable but also rigorously justified by measurable driving dynamics.

2) *Lane-changing Scenario*: The interpretability of LUSPI is further demonstrated in lane-changing scenarios (Fig. 10), where magnitude and trend analyses provide complementary insights into driving behavior semantics. Magnitude analysis quantitatively grounds behavioral interpretations—for instance, the observation that the lane-changing vehicle “maintains a relatively close distance from the lag vehicle” is empirically validated by “average relative distance of 10.1 m”, while “relative speed of 5.5 m/s” confirms it is overtaking the lag vehicle. Trend analysis reveals dynamic behavioral evolution, identifying patterns such as “relative distance increases rapidly” or “relative speed increases slightly”. The synergy of these analyses enables nuanced semantic inference. For example, a moderate initial relative speed coupled with a gradual upward trend suggests the lane-changing vehicle not only travels faster but is also progressively accelerating within a medium-risk range.

This Chain-of-Thought (CoT) reasoning enhances trust in model outputs by transparently linking raw data (e.g., sensor

measurements) to high-level behavioral conclusions. Unlike traditional black-box classifiers, LUSPI leverages the LLM’s knowledge base and contextual reasoning to articulate decision pathways explicitly. This integration achieves superior interpretability without compromising performance—a critical advancement for safety-sensitive applications in autonomous driving.

VII. CONCLUSIONS

This paper presented a novel framework for driving style recognition that leverages sequential driving data augmented with semantic privileged information. The proposed method incorporates DriBehavGPT, an LLM-driven module, to generate human-interpretable descriptions of driving behavior. These semantic features serve as privileged information during training via SVM+, while only standard in-vehicle signals are required for inference, effectively addressing the limitation of conventional approaches that rely on identical input modalities across both phases.

Experimental validation in car-following and lane-changing scenarios demonstrates significant performance gains. In car-following, the framework achieves 90.1% accuracy and 90.2% average F_1 -score, outperforming the SVM baseline by 7.1% and 7.6%, respectively. For lane-changing, it attains 91.5% accuracy and a 91.1% F_1 -score, with improvements of 7.0% and 7.9% over the baseline. These results underscore the efficacy of integrating semantic reasoning into driving behavior analysis, advancing the development of reliable and interpretable intelligent driving systems. Future work will investigate multimodal privileged information (e.g., visual/auditory cues) and extend the framework to urban mixed-traffic environments.

APPENDIX A

The Lagrangian function we construct is as follows:

$$\begin{aligned}
 L(\mathbf{w}, \mathbf{b}, \boldsymbol{\alpha}, \boldsymbol{\beta}) &= \frac{1}{2} (\|\mathbf{w}\|^2 + \gamma \|\mathbf{w}^*\|^2) + C \sum_{i=1}^n (\mathbf{w}^{*\top} \psi(\mathbf{x}_i^*) + b^*) \\
 &- \sum_{i=1}^n \alpha_i \left[y_i (\mathbf{w}^\top \phi(\mathbf{x}_i) + b) - 1 + (\mathbf{w}^{*\top} \psi(\mathbf{x}_i^*) + b^*) \right] \\
 &- \sum_{i=1}^n \beta_i \left[\mathbf{w}^{*\top} \psi(\mathbf{x}_i^*) + b^* \right]
 \end{aligned} \tag{15}$$

Following the principle of Lagrangian duality, we solve the optimization problem by first minimizing the Lagrangian function with respect to $(\mathbf{w}, b, \mathbf{w}^*, b^*)$, and then maximizing the resulting dual function with respect to the Lagrange multipliers $\boldsymbol{\alpha} = [\alpha_1, \dots, \alpha_n]^\top \in \mathbb{R}^n$ and $\boldsymbol{\beta} = [\beta_1, \dots, \beta_n]^\top \in \mathbb{R}^n$.

APPENDIX B

SMO algorithm iteratively maximizes the dual cost function by selecting the best maximally sparse feasible direction in each iteration and updating the corresponding α_i and β_i such

that the dual constraints are also satisfied. The analytical update procedure for Lagrange multipliers proceeds as follows:

$$\alpha_i^{\text{new}} = \alpha_i^{\text{old}} + \eta \frac{\partial \mathcal{L}_d}{\partial \alpha_i} \tag{16}$$

$$\beta_j^{\text{new}} = \beta_j^{\text{old}} + \eta \frac{\partial \mathcal{L}_d}{\partial \beta_j} \tag{17}$$

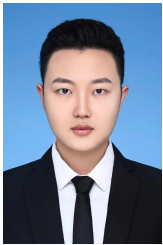
where η is learning rate and \mathcal{L}_d is dual objective function. The algorithm terminates its iterations when the Karush-Kuhn-Tucker (KKT) conditions are satisfied, which occurs when the gradient norm $\|\nabla \mathcal{L}_d\|$ of the dual objective function falls below a predefined threshold ϵ , indicating functional convergence.

REFERENCES

- [1] P. K. Murali, M. Kaboli, and R. Dahiya, “Intelligent in-vehicle interaction technologies,” *Advanced Intelligent Systems*, vol. 4, no. 2, p. 2100122, 2022.
- [2] Y. Kim, S. B. Choi, J. J. Oh, and J. Eo, “Satisfactory driving mode classification based on pedal operation characteristics,” *IEEE Transactions on Intelligent Vehicles*, vol. 9, no. 1, pp. 2988–2998, 2023.
- [3] C.-K. Chau, K. Elbassioni, and C.-M. Tseng, “Drive mode optimization and path planning for plug-in hybrid electric vehicles,” *IEEE Transactions on Intelligent Transportation Systems*, vol. 18, no. 12, pp. 3421–3432, 2017.
- [4] B. Gao, K. Cai, T. Qu, Y. Hu, and H. Chen, “Personalized adaptive cruise control based on online driving style recognition technology and model predictive control,” *IEEE transactions on vehicular technology*, vol. 69, no. 11, pp. 12482–12496, 2020.
- [5] B. Zhu, Y. Jiang, J. Zhao, R. He, N. Bian, and W. Deng, “Typical-driving-style-oriented personalized adaptive cruise control design based on human driving data,” *Transportation research part C: emerging technologies*, vol. 100, pp. 274–288, 2019.
- [6] W. Wang, D. Zhao, J. Xi, D. J. LeBlanc, and J. K. Hedrick, “Development and evaluation of two learning-based personalized driver models for car-following behaviors,” in *2017 American Control Conference (ACC)*. IEEE, 2017, pp. 1133–1138.
- [7] W. Wang and J. Xi, “Study of semi-active suspension control strategy based on driving behaviour characteristics,” *International Journal of Vehicle Design*, vol. 68, no. 1-3, pp. 141–161, 2015.
- [8] W. Wang, J. Xi, C. Liu, and X. Li, “Human-centered feed-forward control of a vehicle steering system based on a driver’s path-following characteristics,” *IEEE transactions on intelligent transportation systems*, vol. 18, no. 6, pp. 1440–1453, 2016.
- [9] W. Wang, D. Zhao, W. Han, and J. Xi, “A learning-based approach for lane departure warning systems with a personalized driver model,” *IEEE Transactions on Vehicular Technology*, vol. 67, no. 10, pp. 9145–9157, 2018.
- [10] D. Dörr, D. Grabengieser, and F. Gauterin, “Online driving style recognition using fuzzy logic,” in *17th international IEEE conference on intelligent transportation systems (ITSC)*. IEEE, 2014, pp. 1021–1026.
- [11] J. Huang, Y. Chen, X. Peng, L. Hu, and D. Cao, “Study on the driving style adaptive vehicle longitudinal control strategy,” *IEEE/CAA Journal of Automatica Sinica*, vol. 7, no. 4, pp. 1107–1115, 2020.
- [12] X. Lin, K. Li, and L. Wang, “A driving-style-oriented adaptive control strategy based pso-fuzzy expert algorithm for a plug-in hybrid electric vehicle,” *Expert Systems with Applications*, vol. 201, p. 117236, 2022.
- [13] K. Liang, Z. Zhao, W. Li, J. Zhou, and D. Yan, “Comprehensive identification of driving style based on vehicle’s driving cycle recognition,” *IEEE Transactions on Vehicular Technology*, vol. 72, no. 1, pp. 312–326, 2022.
- [14] A. Mohammadnazar, R. Arvin, and A. J. Khattak, “Classifying travelers’ driving style using basic safety messages generated by connected vehicles: Application of unsupervised machine learning,” *Transportation research part C: emerging technologies*, vol. 122, p. 102917, 2021.
- [15] X. Tian, Y. Cai, X. Sun, Z. Zhu, Y. Wang, and Y. Xu, “Incorporating driving style recognition into mpc for energy management of plug-in hybrid electric buses,” *IEEE Transactions on Transportation Electrification*, vol. 9, no. 1, pp. 169–181, 2022.

- [16] J. Wang, W. Xu, T. Fu, and R. Jiang, "Recognition of trip-based aggressive driving: A system integrated with gaussian mixture model structured of factor-analysis, and hierarchical clustering," *IEEE Transactions on Intelligent Transportation Systems*, vol. 23, no. 11, pp. 20442–20451, 2022.
- [17] C. Zhang, W. Wang, Z. Ju, Z. Chen, G. Venture, and J. Xi, "An embedded driving style recognition approach: Leveraging knowledge in learning," *IEEE Transactions on Intelligent Vehicles*, 2024.
- [18] Y. Zhong, "A theory of semantic information," *China communications*, vol. 14, no. 1, pp. 1–17, 2017.
- [19] S. Chen, Z. Jian, Y. Huang, Y. Chen, Z. Zhou, and N. Zheng, "Autonomous driving: cognitive construction and situation understanding," *Science China Information Sciences*, vol. 62, pp. 1–27, 2019.
- [20] R. Yang, X. Zhang, A. Fernandez-Laaksonen, X. Ding, and J. Gong, "Driving style alignment for llm-powered driver agent," in *2024 IEEE/RSJ International Conference on Intelligent Robots and Systems (IROS)*. IEEE, 2024, pp. 11 318–11 324.
- [21] B. Min, H. Ross, E. Sulem, A. P. B. Veysch, T. H. Nguyen, O. Sainz, E. Agirre, I. Heintz, and D. Roth, "Recent advances in natural language processing via large pre-trained language models: A survey," *ACM Computing Surveys*, vol. 56, no. 2, pp. 1–40, 2023.
- [22] J. Wei, X. Wang, D. Schuurmans, M. Bosma, F. Xia, E. Chi, Q. V. Le, D. Zhou *et al.*, "Chain-of-thought prompting elicits reasoning in large language models," *Advances in neural information processing systems*, vol. 35, pp. 24 824–24 837, 2022.
- [23] D. Pechony and V. Vapnik, "On the theory of learning with privileged information," *Advances in neural information processing systems*, vol. 23, 2010.
- [24] M. A. L. Ralph, E. Jefferies, K. Patterson, and T. T. Rogers, "The neural and computational bases of semantic cognition," *Nature reviews neuroscience*, vol. 18, no. 1, pp. 42–55, 2017.
- [25] Y. Xia, M. Geng, Y. Chen, S. Sun, C. Liao, Z. Zhu, Z. Li, W. Y. Ochieng, P. Angeloudis, M. Elhajj *et al.*, "Understanding common human driving semantics for autonomous vehicles," *Patterns*, 2023.
- [26] E. Gulian, G. Matthews, A. I. Glendon, D. Davies, and L. Debney, "Dimensions of driver stress," *Ergonomics*, vol. 32, no. 6, pp. 585–602, 1989.
- [27] D. J. French, R. J. West, J. Elander, and J. M. Wilding, "Decision-making style, driving style, and self-reported involvement in road traffic accidents," *Ergonomics*, vol. 36, no. 6, pp. 627–644, 1993.
- [28] W. Wang, J. Xi, and D. Zhao, "Driving style analysis using primitive driving patterns with bayesian nonparametric approaches," *IEEE Transactions on Intelligent Transportation Systems*, vol. 20, no. 8, pp. 2986–2998, 2018.
- [29] Y. Chen, G. Li, S. Li, W. Wang, S. E. Li, and B. Cheng, "Exploring behavioral patterns of lane change maneuvers for human-like autonomous driving," *IEEE Transactions on Intelligent Transportation Systems*, vol. 23, no. 9, pp. 14 322–14 335, 2021.
- [30] C. Zhang, W. Wang, Z. Chen, J. Zhang, L. Sun, and J. Xi, "Shareable driving style learning and analysis with a hierarchical latent model," *IEEE Transactions on Intelligent Transportation Systems*, vol. 25, no. 9, pp. 11 471–11 484, 2024.
- [31] V. Vapnik and A. Vashist, "A new learning paradigm: Learning using privileged information," *Neural networks*, vol. 22, no. 5-6, pp. 544–557, 2009.
- [32] F. Li, L. Zhang, Z. Liu, J. Lei, and Z. Li, "Multi-frequency representation enhancement with privilege information for video super-resolution," in *Proceedings of the IEEE/CVF International Conference on Computer Vision*, 2023, pp. 12 814–12 825.
- [33] X. Yang, M. Wang, and D. Tao, "Person re-identification with metric learning using privileged information," *IEEE Transactions on Image Processing*, vol. 27, no. 2, pp. 791–805, 2017.
- [34] G. Ortiz-Jimenez, M. Collier, A. Nawalgaria, A. N. D'Amour, J. Berent, R. Jenatton, and E. Kokiopoulou, "When does privileged information explain away label noise?" in *International Conference on Machine Learning*. PMLR, 2023, pp. 26 646–26 669.
- [35] M. Ganaie and M. Tanveer, "Ensemble deep random vector functional link network using privileged information for alzheimer's disease diagnosis," *IEEE/ACM Transactions on Computational Biology and Bioinformatics*, 2022.
- [36] Z. Gao, J. Chung, M. Abdelrazek, S. Leung, W. K. Hau, Z. Xian, H. Zhang, and S. Li, "Privileged modality distillation for vessel border detection in intracoronary imaging," *IEEE transactions on medical imaging*, vol. 39, no. 5, pp. 1524–1534, 2019.
- [37] Z. Shi and T.-K. Kim, "Learning and refining of privileged information-based rns for action recognition from depth sequences," in *Proceedings of the IEEE conference on computer vision and pattern recognition*, 2017, pp. 3461–3470.
- [38] F. Liu, X. Xu, T. Zhang, K. Guo, and L. Wang, "Exploring privileged information from simple actions for complex action recognition," *Neurocomputing*, vol. 380, pp. 236–245, 2020.
- [39] E. Sabeti, J. Drews, N. Reamaroon, E. Warner, M. W. Sjoding, J. Gryak, and K. Najarian, "Learning using partially available privileged information and label uncertainty: Application in detection of acute respiratory distress syndrome," *IEEE journal of biomedical and health informatics*, vol. 25, no. 3, pp. 784–796, 2020.
- [40] D. Fu, X. Li, L. Wen, M. Dou, P. Cai, B. Shi, and Y. Qiao, "Drive like a human: Rethinking autonomous driving with large language models," in *Proceedings of the IEEE/CVF Winter Conference on Applications of Computer Vision*, 2024, pp. 910–919.
- [41] C. Cui, Y. Ma, X. Cao, W. Ye, and Z. Wang, "Drive as you speak: Enabling human-like interaction with large language models in autonomous vehicles," in *Proceedings of the IEEE/CVF Winter Conference on Applications of Computer Vision*, 2024, pp. 902–909.
- [42] X. Li and Y. Sun, "Stock intelligent investment strategy based on support vector machine parameter optimization algorithm," *Neural Computing and Applications*, vol. 32, no. 6, pp. 1765–1775, 2020.
- [43] Y. Xiao, H. Wang, and W. Xu, "Parameter selection of gaussian kernel for one-class svm," *IEEE transactions on cybernetics*, vol. 45, no. 5, pp. 941–953, 2014.
- [44] D. Pechony, R. Izmailov, A. Vashist, and V. Vapnik, "Smo-style algorithms for learning using privileged information," *Dmin*, vol. 10, pp. 235–241, 2010.
- [45] J. Achiam, S. Adler, S. Agarwal, L. Ahmad, I. Akkaya, F. L. Aleman, D. Almeida, J. Altenschmidt, S. Altman, S. Anadkat *et al.*, "Gpt-4 technical report," *arXiv preprint arXiv:2303.08774*, 2023.
- [46] J. Elander, R. West, and D. French, "Behavioral correlates of individual differences in road-traffic crash risk: An examination of methods and findings," *Psychological bulletin*, vol. 113, no. 2, p. 279, 1993.
- [47] H. Bellem, B. Thiel, M. Schrauf, and J. F. Krems, "Comfort in automated driving: An analysis of preferences for different automated driving styles and their dependence on personality traits," *Transportation research part F: traffic psychology and behaviour*, vol. 55, pp. 90–100, 2018.
- [48] C.-T. Lin, Y. Tian, Y.-K. Wang, T.-T. N. Do, Y.-L. Chang, J.-T. King, K.-C. Huang, and L.-D. Liao, "Effects of multisensory distractor interference on attentional driving," *IEEE transactions on intelligent transportation systems*, vol. 23, no. 8, pp. 10 395–10 403, 2022.
- [49] N. Reimers, "Sentence-bert: Sentence embeddings using siamese bert-networks," *arXiv preprint arXiv:1908.10084*, 2019.
- [50] T. Mikolov, "Efficient estimation of word representations in vector space," *arXiv preprint arXiv:1301.3781*, vol. 3781, 2013.
- [51] J. Pennington, R. Socher, and C. D. Manning, "Glove: Global vectors for word representation," in *Proceedings of the 2014 conference on empirical methods in natural language processing (EMNLP)*, 2014, pp. 1532–1543.
- [52] J. Healy and L. McInnes, "Uniform manifold approximation and projection," *Nature Reviews Methods Primers*, vol. 4, no. 1, p. 82, 2024.
- [53] R. Krajewski, J. Bock, L. Kloeker, and L. Eckstein, "The highd dataset: A drone dataset of naturalistic vehicle trajectories on german highways for validation of highly automated driving systems," in *2018 21st International Conference on Intelligent Transportation Systems (ITSC)*. IEEE, 2018, pp. 2118–2125.
- [54] X. Chen, M. Zhu, K. Chen, P. Wang, H. Lu, H. Zhong, X. Han, X. Wang, and Y. Wang, "Follownet: a comprehensive benchmark for car-following behavior modeling," *Scientific data*, vol. 10, no. 1, p. 828, 2023.
- [55] M. Zhu, X. Wang, and Y. Wang, "Human-like autonomous car-following model with deep reinforcement learning," *Transportation research part C: emerging technologies*, vol. 97, pp. 348–368, 2018.
- [56] X. Wang, R. Jiang, L. Li, Y. Lin, X. Zheng, and F.-Y. Wang, "Capturing car-following behaviors by deep learning," *IEEE Transactions on Intelligent Transportation Systems*, vol. 19, no. 3, pp. 910–920, 2017.
- [57] B. Higgs and M. Abbas, "Segmentation and clustering of car-following behavior: Recognition of driving patterns," *IEEE Transactions on Intelligent Transportation Systems*, vol. 16, no. 1, pp. 81–90, 2014.
- [58] Y. Xing, C. Lv, H. Wang, D. Cao, and E. Velenis, "An ensemble deep learning approach for driver lane change intention inference," *Transportation Research Part C: Emerging Technologies*, vol. 115, p. 102615, 2020.
- [59] V. Mahajan, C. Katrakazas, and C. Antoniou, "Prediction of lane-changing maneuvers with automatic labeling and deep learning," *Transportation research record*, vol. 2674, no. 7, pp. 336–347, 2020.

- [60] J. Zhang, G. Li, Z. Deng, H. Yu, J. P. Huissoon, and D. Cao, "Interaction-aware cut-in behavior prediction and risk assessment for autonomous driving," *IFAC-PapersOnLine*, vol. 53, no. 5, pp. 656–663, 2020.
- [61] G. Yan, H. Yu, C. Zhang, and J. Xi, "Interaction-awareness based intention inference of lag vehicle in lane changing decision-making process for autonomous driving," in *2023 IEEE 6th International Conference on Industrial Cyber-Physical Systems (ICPS)*. IEEE, 2023, pp. 1–8.
- [62] S. Yang, W. Wang, C. Lu, J. Gong, and J. Xi, "A time-efficient approach for decision-making style recognition in lane-changing behavior," *IEEE Transactions on Human-Machine Systems*, vol. 49, no. 6, pp. 579–588, 2019.
- [63] G. Asaithambi and G. Shrivani, "Overtaking behaviour of vehicles on undivided roads in non-lane based mixed traffic conditions," *Journal of traffic and transportation engineering (English edition)*, vol. 4, no. 3, pp. 252–261, 2017.
- [64] K. Vogel, "A comparison of headway and time to collision as safety indicators," *Accident analysis & prevention*, vol. 35, no. 3, pp. 427–433, 2003.
- [65] E. Schubert, J. Sander, M. Ester, H. P. Kriegel, and X. Xu, "Dbscan revisited, revisited: why and how you should (still) use dbscan," *ACM Transactions on Database Systems (TODS)*, vol. 42, no. 3, pp. 1–21, 2017.



Zhaokun Chen received the B.S. degree in Intelligent Automotive Engineering from the Harbin Institute of Technology, Weihai, China, in 2022. He is currently working toward the Ph.D. degree in mechanical engineering with the Beijing Institute of Technology, Beijing, China. His research interests include driving behavior analysis, human driver models, driving style recognition, and human-centered driving.



Chaopeng Zhang received B.S. degree in Mechanical Engineering from Beijing Institute of Technology, Beijing, China, in 2019, where he is currently working toward the Ph.D. degree in mechanical engineering. He is now studying at the Department of Mechanical Engineering, University of Tokyo. His research interests include human factors in intelligent vehicles, human driver models, driving style recognition, and driving intention recognition.



Xiaohan Li received the B.S. degree in Automotive Engineering from Jilin University, Changchun, China, in 2025. She is currently working toward the M.S. degree in mechanical engineering with the Beijing Institute of Technology, Beijing, China. Her research interests include driving style recognition, human factors in intelligent vehicles, and human intention recognition.



Wenshuo Wang (SM'15-M'18) received his Ph.D. degree in mechanical engineering from the Beijing Institute of Technology (BIT) in 2018. Presently, he is a Full Professor at the School of Mechanical Engineering, BIT, Beijing, China. Prior to his role at BIT, he completed Postdoctoral fellowships at McGill University, Carnegie Mellon University (CMU), and UC Berkeley between 2018 and 2023. Furthermore, from 2015 to 2018, he served as a Research Assistant at UC Berkeley and the University of Michigan, Ann Arbor. His research interests focus on Bayesian nonparametric learning, human driver model, human-vehicle interaction, ADAS, and autonomous vehicles.



Gentiane Venture is a French Robotist working in academia in Tokyo. She is a professor at the University of Tokyo and a cross-appointed fellow with AIST. She obtained her MSc and PhD from Ecole Centrale/University of Nantes in 2000 and 2003 respectively. She worked at CEA, France in 2004 and for 5 years at the University of Tokyo, Japan. In 2009 she started with Tokyo University of Agriculture and Technology where she established an international research group working on human science and robotics, before moving to her present affiliation in 2022. With her group, she conducts theoretical and applied research on motion dynamics, robot control, and non-verbal communication to study the meaning of living with robots. Her work is highly interdisciplinary, collaborating with therapists, psychologists, neuroscientists, sociologists, philosophers, ergonomists, artists, and designers.



Junqiang Xi received the B.S. degree in automotive engineering from the Harbin Institute of Technology, Harbin, China, in 1995, and the Ph.D. degree in vehicle engineering from the Beijing Institute of Technology (BIT), Beijing, China, in 2001. In 2001, he joined the State Key Laboratory of Vehicle Transmission, BIT. During 2012–2013, he made research as an Advanced Research Scholar in Vehicle Dynamic and Control Laboratory, Ohio State University, Columbus, OH, USA. He is currently a Professor and Director of Automotive Research Center in BIT. His research interests include vehicle dynamic and control, powertrain control, mechanics, intelligent transportation system, and intelligent vehicles.